

CHAPTER 6

OPM, SYNCHROTRON X-RAY DIFFRACTION AND DIELECTRIC STUDY ON A CHIRAL BIPHENYL CARBOXYLATE

Part of the work has been published in Materials Research Express., Vol. 1: pp. 035101–035113, 2014.

6.1 INTRODUCTION

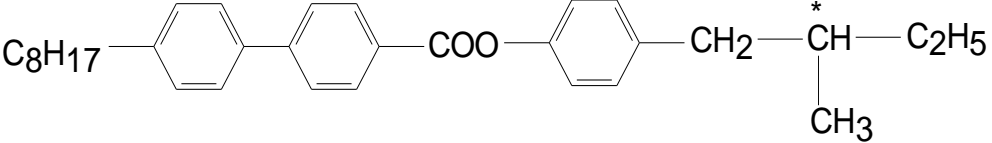
Liquid crystals are an important subclass of soft condensed matter and can be broadly described as ordered fluids formed from geometrically anisotropic molecules. In these self-assembling media on nanoscale level molecular ordering is intermediate between that of the crystalline solid and the isotropic liquid phases. There may be only orientational ordering (nematic) or one dimensional positional ordering with layered structure (smectic). Considering tilt of the constituent molecular long axis (known as director which is the average direction in which the molecules point) from the layer normal, hexatic bond orientational ordering, translational ordering within the smectic layers and interlayer correlation of this ordering [1,2] they are classified into SmA, SmC, SmB_{hex}, SmF, SmI, SmB_{cryst}, SmG, SmJ (SmG'), SmE, SmH and SmK (SmH') where in SmA, SmB_{hex}, SmB_{cryst} and SmE phases molecules are normal to the layers and in the remaining phases molecules are tilted within the layers. When the constituent molecules are chiral and the system is not racemic, tilted smectic phases are designated as SmC*, SmI*, etc; so also the nematic phase as N* (cholesteric phase). In some chiral systems another phase, known as blue phase, appears between the cholesteric phase (N*) and the isotropic phase in a narrow temperature range. Although all these phases are not usually observed in a single compound but some systems exhibit a large variety of them. Liquid crystals are, therefore, considered as an ideal system for studying the phenomena of phase transitions and critical behaviour. The chiral tilted phases also show ferroelectric behavior when the constituent molecules possess permanent dipole moment perpendicular to long axis and close to the chiral centre [3], being the only example of fluid ferroelectrics. However, when the helical structure is stable in free bulk sample, the tilt directions are continuously degenerate and hence there exists no net polarization. In a thin surface stabilized ferroelectric liquid crystal (SSFLC) cell, the helical structure is unwound spontaneously; continuous degeneracy is lifted and results in bistability [4]. Liquid crystalline compound containing blue phase has a number of interesting properties. As mentioned earlier, since blue phases are liquid phases, they exhibit a non-zero elastic shear modulus. The magnitude of the elastic shear modulus is about 10⁶ times smaller than that of a conventional solid [5]. In addition, the blue phases possess higher viscosity than either the helical or isotropic phase [5]. The blue phases have unique optical properties and some physical properties rarely associated with liquids due to their complicated lattice structure of double-twist tubes which make blue phases so fascinating and interesting. Now a days the blue

phase technology is used to obtain a better display of moving images (with frame rates of 100–120 Hz) to improve the temporal response of LCDs. Keeping these in view, a chiral liquid crystal system has been chosen to investigate which exhibit a large variety of tilted hexatic phases as well as blue phases. This is the only non-fluorinated compound investigated in the present dissertation.

6.2 COMPOUND STUDIED

Phase behavior, structure and dynamics of the chiral compound (S)-4-(2'-methylbutyl) phenyl-4-(n-octyl) biphenyl-4-carboxylate (abbreviated as MPOBC) has been studied by employing optical polarizing microscopy, synchrotron X-ray diffraction and frequency dependent dielectric spectroscopy techniques. Molecular structure of the investigated compound along with its abbreviated name and transition temperature (in °C) are given in the table 6.1.

Table 6.1: Molecular structure and phase transition temperatures of MPOBC

Name	Molecular structure with transition temperature
MPOBC	 <p style="text-align: center;">Cr 48 SmG* 63 SmJ* 65 SmF* 67 SmI* 71 SmC* 81 SmA* 136 N* 139 BP* 140 Iso</p>

The compound exhibits, other than crystalline and isotropic phases, four tilted hexatic (SmG^* , SmJ^* , SmF^* , SmI^*), one tilted synclonic phase (SmC^*), one orthogonal smectic phase (SmA^*), cholesteric phase (N^*) and blue phase (BP^*).

6.3 EXPERIMENTAL METHODS

Phase behavior and transition temperatures of MPOBC have been investigated by studying its topological defect structures under an Olympus BX41 polarizing microscope equipped with CCD camera, temperature regulation was made, within $\pm 0.1^\circ\text{C}$, using Mettler FP82 central processor and FP84 hot stage.

Mesophase structural investigation was made using synchrotron radiation facility (PETRA III beamline at P07 Physics Hutch station) at DESY, Hamburg. For this study, sample was taken in a Lindemann glass capillary of diameter 1.0 mm and very slowly cooled down from isotropic phase to the desired temperature to get aligned sample. 50 images of exposure time 0.2s was grabbed and averaged to get one diffraction image and such five images were collected at a particular temperature. All the physical parameters were averaged over these five image data. A Perkin Elmer 2D detector of pixel size $200 \times 200 \mu\text{m}$ and total size $400 \times 400 \text{ mm}$ was used for image grabbing which was placed at 3.3 m away from the sample. QXRD program for PE Area Detectors (G. Jennings, version 0.9.8, 64 bit) was used for data acquisition and also for analyzing the images. Images were integrated using a step size of 0.002 to get intensity versus wave vector (Q) distribution.

Relaxation behavior of MPOBC was studied by measuring frequency dependent complex dielectric permittivity using a computer controlled impedance analyzer HIOKI 3532-50 (50Hz–5 MHz). Polyimide-coated homogeneous (HG) cells in the form of a parallel plate capacitor with low resistivity (about $20 \Omega/\square$) indium tin oxide (ITO) electrodes of $\sim 5 \mu\text{m}$ cell gap were used. The cells were filled by capillary action with samples in isotropic state and cell temperature was maintained within $\pm 0.1^\circ\text{C}$ using Eurotherm 2216e temperature controller. Very slow regulated cooling of the sample was made to get proper alignment. To find the dielectric increment and relaxation frequency of a particular mode, observed dielectric spectra, as mentioned in chapter 2, were fitted to the following complex dielectric permittivity proposed by Cole-Cole [6,7,8], which was modified to take into account the low and high frequency parasitic effects:

$$\varepsilon^* = \varepsilon' - i\varepsilon'' = \varepsilon_\infty + \sum_k \frac{\Delta\varepsilon_k}{1 + (i\omega\tau_k)^{1-\alpha_k}} - i \frac{\sigma}{\omega\varepsilon_0}$$

where $\Delta\varepsilon_k = \varepsilon_0 - \varepsilon_\infty$ is the dielectric increment, ε_0 and ε_∞ being the real part of the low and high frequency limit dielectric permittivities, τ_k is the relaxation time (inverse of critical angular frequency) and α_k is the asymmetry parameter signifying deviation from Debye type behavior of k-th mode relaxation process. σ is the conductivity of the cell due to charge impurities which contributes mainly in low frequency region.

Spontaneous polarization (P_S) was measured as a function of temperature by the reversal current method [9] using a triangular wave at 10 Hz obtained from an Agilent 3320A function generator. The amplitude of the applied voltage was 20 V_{pp}. A digital oscilloscope ((Tektronix TDS 2012B) was used to record the voltage drop across a standard resistor in series with the cell as a function of time. The area under the curve was determined from the stored image after creating an appropriate base line following procedure described before [10]. P_S was calculated using the expression $P_S = \int V dt / (2AR)$ where A is the active area of the cell and R is the resistance used to record the voltage–time curve.

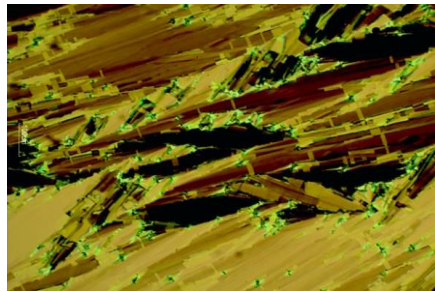
Since in an ac field the molecules switch around an imaginary cone through twice the tilt angle there by reversing the sign of the P_S , tilt of the molecules in smectic layers was determined by measuring the angle of rotation of the analyzer between two extinction conditions while observing, under polarizing microscope, switching of the molecules subjected to a 10 mHz 40 volt square wave pulse. This tilt is referred to as optical tilt. From synchrotron data tilt was also determined which is known as X-ray tilt.

6.4 RESULTS AND DISCUSSIONS

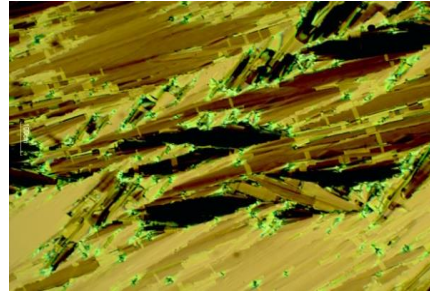
6.4.1 Optical Polarizing Microscopy

The compound MPOBC exhibits richly polymorphic behavior – as many as ten different phases are observed. Photo micrographs of textures of different phases observed under planar anchoring condition are shown in Figure 6.1. Molecules of MPOBC contain an asymmetric C* atom rendering chirality while the carbonyl (–C=O) functional group provides a transverse permanent electric dipole moment. Variant of mosaic textures are observed in SmG* and SmJ*

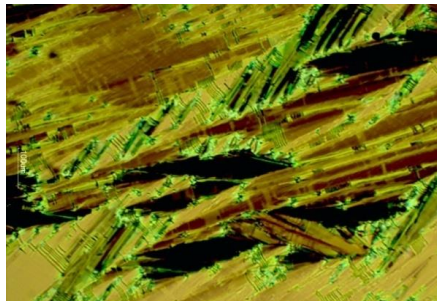
phases, they differ only slightly in colour; there is no indication of helical structure. Within the individual grains the optic axis is oriented uniformly and homogeneously, while discontinuous direction changes of the long molecular axes are encountered advancing from grain to grain, leading to differently coloured mosaic phases [11]. These two phases are soft crystal like with pseudo-hexagonal packing within the smectic layers, with long range bond orientational order as well as long range interlayer correlation. They differ only in the direction of tilt of the molecules, in SmG^* the tilt is towards the side of the hexagon while in SmJ^* it is towards the apex of the hexagon [12,13]. In the next two higher temperature smectic phases, SmF^* and SmI^* , textures change from the above phases, indication of helicoidal structure is now visible in the form of parallel equidistant lines, more in SmI^* than in SmF^* . Measured pitch values in the two phases estimated from the separation of helical lines are 5-10 μm . Unlike in MPOBC, usually only SmI^* phase is observed below SmC^* phase. In these two phases the molecular packing is also pseudo-hexagonal, but both the bond orientational order and the interlayer correlation are quasi long range in nature, in SmF^* the tilt is towards the side of the hexagon while in SmI^* it is towards the apex of the hexagon [14]. In SmC^* phase the texture is uniform throughout the field of view and existence of helicoidal structure is also evident throughout the sample. It transforms to typical fan shaped texture in orthogonal SmA^* phase, to oily streaks texture in cholesteric (N^*) phase, appearance of oily streaks at the expense of fan shaped texture is clearly seen at SmA-N^* transition. Blue coloured platelet texture is observed in blue phase. This is definitely not BPIII^* phase or “fog phase”, it is difficult to ascertain whether it is a BPI^* or BPII^* phase both of which are cubic phases, the former being simple cubic whereas the later is body centered cubic. But since the lower temperature phase is a cholesteric phase this phase is likely to be a BPI^* phase [11, 15].



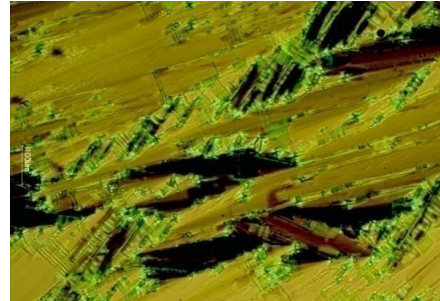
SmG* Phase (50°C)



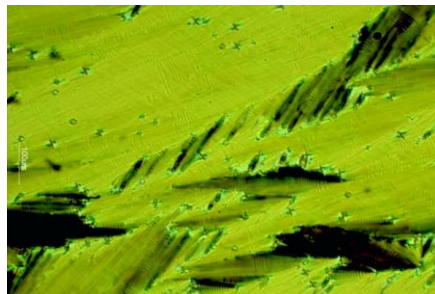
SmJ* Phase (64°C)



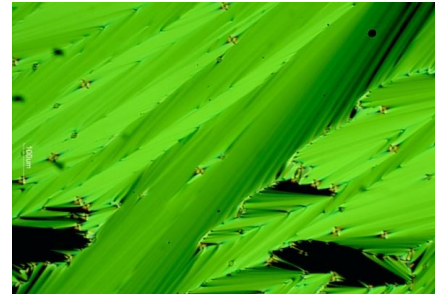
SmF* Phase (66°C)



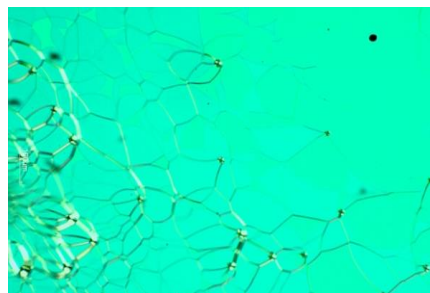
SmI* Phase (69°C)



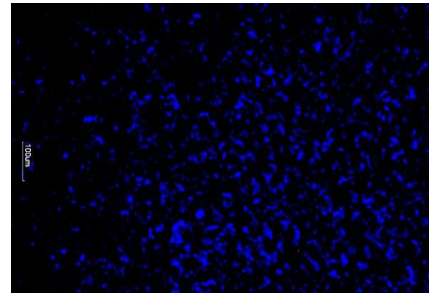
SmC* Phase (75°C)



SmA* Phase (100°C)



N* Phase (138°C)



Blue Phase (139.5°C)

Figure 6.1: Observed textures in MPOBC in different phases.

It may be of interest to point out that molecular structures of the compounds have pronounced effect on their phase behavior. While the present compound MPOBC shows eight different liquid crystalline phases, the compound DOBAMBC, the first ferroelectric liquid crystal [3], was having different molecular structure [$C_{10}H_{21}O.Ph.CHN.Ph.CH.CH.COO.CH_2.CH(CH_3).C_2H_5$] from MPOBC, exhibits only one ferroelectric (SmC^*) and one paraelectric phase (SmA^*); on the other hand in the first antiferroelectric liquid crystal MHPOBC, having core structure similar to MPOBC, [$C_8H_{17}O.Ph.Ph.COO.Ph.COO.CH(CH_3).C_6H_{13}$], three sub phases of ferroelectric SmC^* are found to exist between anticlinic SmC^*_A and orthogonal SmA^* phases [16]. When the six end carbon atoms of alkoxy chain of MHPOBC are fluorinated antiferroelectric phase is suppressed [10].

6.4.2 X-Ray Study

Since conventional X-ray scattering is not sensitive to the local environment of a molecule it cannot distinguish smectic liquid crystal phases that differ only with respect to the orientation of the molecules in successive layers like antiferroelectric SmC^*_A , ferroelectric SmC^* and various intermediate ferroelectric phases but it can distinguish smectic phases that differ with respect to the packing of molecules within the smectic layers. Although no external field, magnetic or electric, was used to align the sample, partial alignment was achieved due to surface interaction, with molecular axes perpendicular to beam direction. Diffraction photographs obtained in different phases are shown in Figure 6.2. Transition temperatures seen from X-ray study are found to be shifted to higher side by 1 to 2 degrees than those observed from optical microscopy study since two different temperature baths were used. In SmG^* phase one strong inner ring is present with quite strong second order diffraction feature signifying long range positional order across the smectic layers. One very strong outer ring with two distinct satellites on both sides is also observed in this phase characterizing two dimensional positional ordering within the smectic layers as depicted in Figure 6.3. Correlation length (ξ), defined as $\xi=2\pi/FWHM$

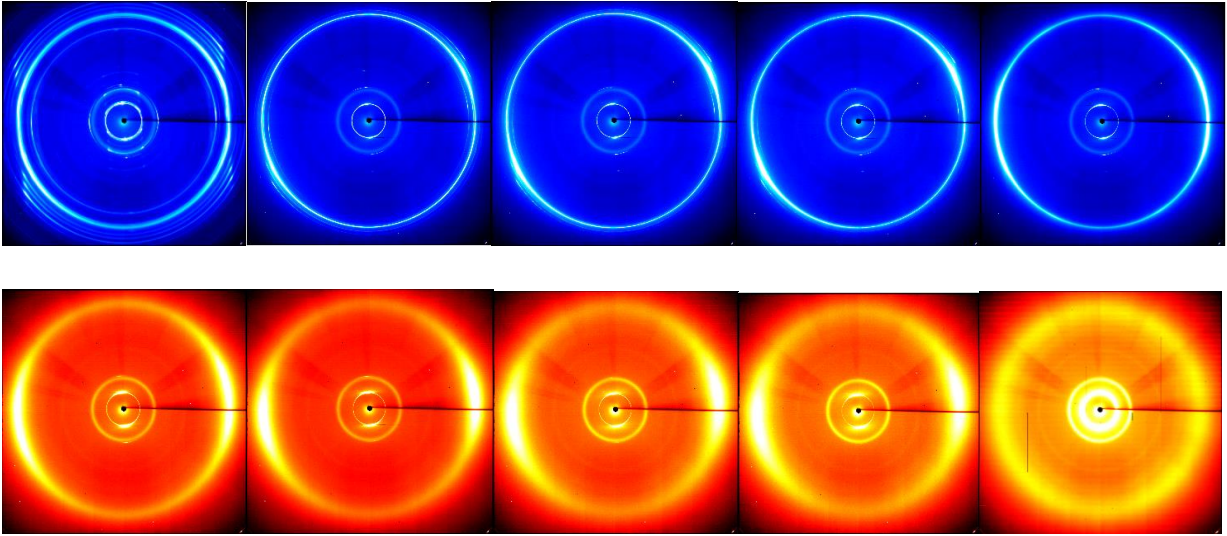


Figure 6.2: Diffraction photographs in Crystal, SmG^{*}, SmJ^{*}, SmF^{*}, SmI^{*}, SmC^{*}, SmA^{*}, N^{*}, BP^{*} and isotropic phases

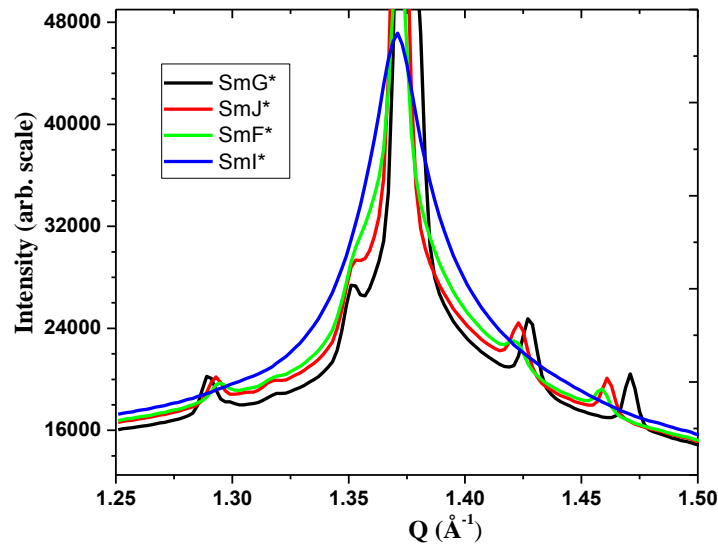


Figure 6.3: Profile of wide angle diffraction peak depicting ordering within smectic planes in hehatic phases at 55^oC (SmG^{*}), 64^oC (SmJ^{*}), 66^oC (SmF^{*}) and 68^oC (SmI^{*})

where FWHM is the full width at half maxima in scattering vector (Q) of the relevant Bragg peak, is found to be 145 nm across the smectic layers and 65 nm within the layers. Diffraction features remain almost same in SmJ^{*} phase, only the second order of the inner peak and the

satellites of the outer peak become less prominent and ξ decreases slightly both across (140 nm) and within the smectic layers (59 nm), decrease in molecular tilt angle is also observed. Quite strong second order inner diffraction peak (although less than those in SmG^* and SmJ^* phases) is observed but the satellites of the outer peak are very weak in SmF^* phase which means correlation across the smectic layers reduces slightly (134 nm) but within the layers it becomes half (30 nm). In SmI^* phase, a 30° rotation of outer maxima is distinctly observed which gives direct evidence of change of tilt direction of the molecules from the edge of the pseudo-hexagonal net towards its apex. Correlation lengths also reduce to 125 nm and 22 nm across and within the layers respectively. In-plane correlation lengths ranging from 5 to 20 nm has been reported from quasielastic light scattering experiment on thin film of SmI^* phase and also from X-ray measurements [17,18] in this compound. In ferroelectric SmC^* and paraelectric SmA^* phases correlation lengths across the smectic layers decreases slightly to 118 nm and 116 nm respectively, no positional ordering is observed within the layers and ξ reduces drastically to about 3 nm in both phases. Same trend is observed in cholesteric (N^*) phase. But in blue phase, correlation length along the director increases substantially to 134 nm from 113 nm in cholesteric phase. This is expected since the blue phase structures involve a twist of the director extending not only in one direction, such as in cholesteric phase, but in both directions perpendicular to the director generating what is known as double twist structure [19]. However, observed correlation length for MPOBC is substantially large than that observed in $\text{BP}_{\text{Sm}1}$ and $\text{BP}_{\text{Sm}2}$ phases (58 nm) of a different chiral compound [19]. Clear discontinuities are also observed at all phase transitions in d_{001} smectic layer spacing as shown in Figure 6.4. Present study therefore clearly depicts the temperature evolution of the different tilted hexatic smectic phases along with cholesteric and blue phase in a single compound. Tilt (τ) of the molecules with respect to smectic layer normal has also been calculated using the relation, $\tau = \arccos(d/d_A)$ where d_A is average layer spacing in SmA^* phase. Molecular tilt is found to decrease with temperature, in SmG^* and SmJ^* phases from 16.5° to 14.6° however, at the onset of SmF^* phase it increases slightly to 14.9° and then decreases up to 12.5° till the end of SmI^* phase. Thus discontinuous change in tilt is observed only when molecules change orientations from apex to edge of the in-plane hexagonal net. At the onset of SmC^* phase it again jumps up and then decreases with temperature as in previous hexatic smectic phases. Temperature variation of tilt is shown in Figure 6.5. It is further noted that tilt angle (12.54°) calculated as above at 72°C is found to be equal to that measured

directly from the film (12.5°) which justifies calculation of tilt angle, at least in SmC^* phase, taking average d_A . Our measured value in SmJ^* phase (14.6°) is less than reported (19°) from extinction measurement in a SSFLC cell under a polarizing microscope [20].

Average intermolecular distance (D), determined from outer peak (in SmG^* , SmJ^* , SmF^* and SmI^* phases from the main outer peak) is found to increase monotonically from 4.58 \AA to 4.79 \AA . However, no discontinuity is observed in D as observed in d_{001} spacing. D values observed in MPOBC is substantially less than the values (5.87 \AA and 6.89 \AA) observed in chiral terphenyl compounds having oligomethylene spacer and ester group in the chain part, discussed in chapter 5.

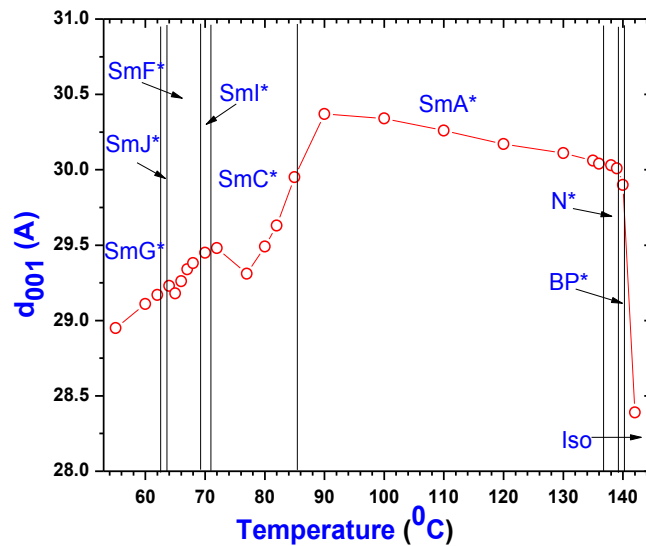


Figure 6.4: Layer spacing in smectic phases and apparent molecular length in cholesteric, blue and isotropic phases.

6.4.3 Optical Tilt

Optical tilt of the molecules in different phases has also been determined and depicted in Figure 6.5. Distinct discontinuities are observed at the phase transition points. In SmG^* phase tilt (τ) increases from 14.7° to 19.8° with temperature, in SmJ^* phase it increases further from 20.0° to 21.0° . However, in SmF^* phase tilt suddenly decreases to 17.0° and continue to decrease up to

13° . In SmI^* phase τ increases to 16.0° and then decreases to 14.8° . In SmC^* phase it again increases to 19° and then decreases with temperature to 3° . Thus except in SmG^* and SmJ^* phases molecular tilt decreases with temperature. Unlike in X-ray tilt clear discontinuities are observed in optical tilt at all transitions except at SmG^* - SmJ^* transition. Optical tilt reflects the angle between the direction of molecular core and the layer normal, since the principal axis of indicatrix coincides with the core direction. On the other hand, X-ray tilt gives the average direction of total populations of electrons of the molecules. Thus X-ray tilt is usually found to be larger than optical tilt and in the present compound MPOBC it is found to be true in SmC^* phase as reported in systems described in chapter 5 and as reported earlier in other systems [8,21], however, in higher ordered tilted phases (SmI^* and SmJ^*) opposite behavior is observed, such behavior has also been reported in SmC^* phase [22,23]. A crossover is found in SmG^* phase.

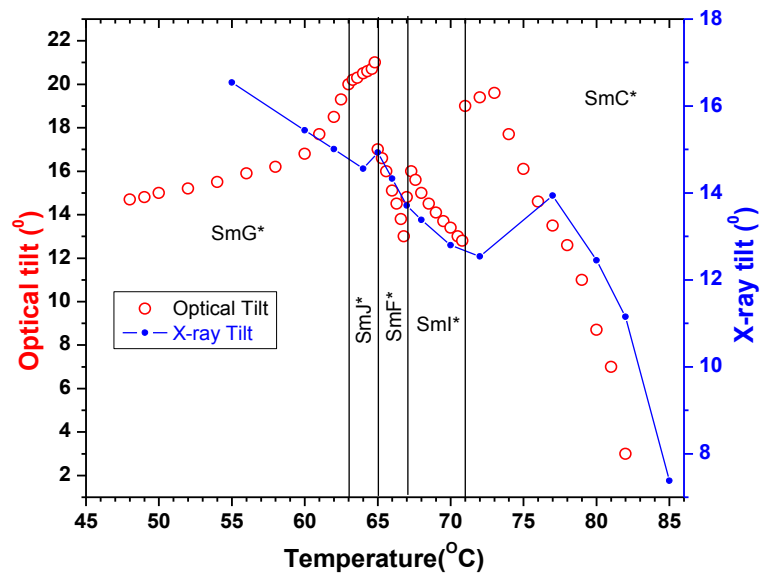


Figure 6.5: Temperature dependence of X-ray and optical tilt of MPOBC.

6.4.4 Spontaneous Polarization (P_s)

Measuring depolarization current using triangular wave method P_s has been measured in ferroelectric SmC^* phase. Although any chiral tilted phase may possess, due to symmetry consideration, spontaneous polarization, we could measure P_s only in SmC^* phase. No previous report on P_s measurement in SmG^* and SmJ^* phases are available, but P_s in SmI^* phase was reported [24]. In a two ring perfluorinated compound it was found that SmI^* phase exhibits almost 3 times larger spontaneous polarization than the high temperature ferroelectric SmC^* phase when the applied field is very high but at lower field P_s was less than in SmC^* phase. From optimized geometry of the molecule, obtained by molecular mechanics calculation using PM3 method of software Hyperchem (shown in Figure 6.6), dipole moment of the molecules is found to be 2.06 Debye which is rather small compared to other chiral liquid crystal forming compounds; for example dipole moments of 4F3R and 4F6R, discussed in chapter 5, are 4.25 Debye and 5.75 Debye respectively [8]. However, P_s was found to be quite high, maximum value being 237 nC/cm^2 and found to fall off rapidly with temperature. Heating and cooling data was found to be almost identical and data obtained during cooling are shown in Figure 6.7. Although increase of molecular lateral dipole moment normally leads to increased P_s but molecular rotations around their long axes and various intramolecular rotations in the mesophase play important role in the macroscopic P_s values.

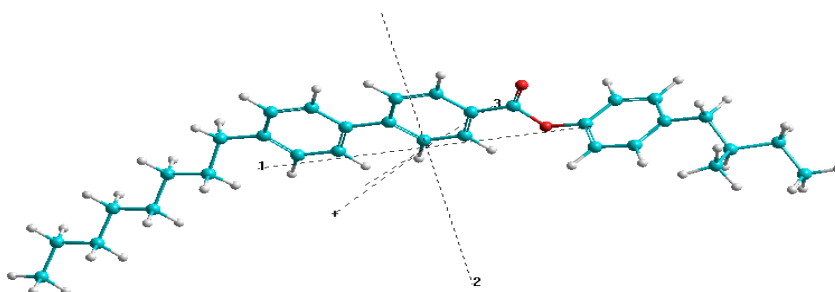


Figure 6.6: Optimized structure of MPOBC

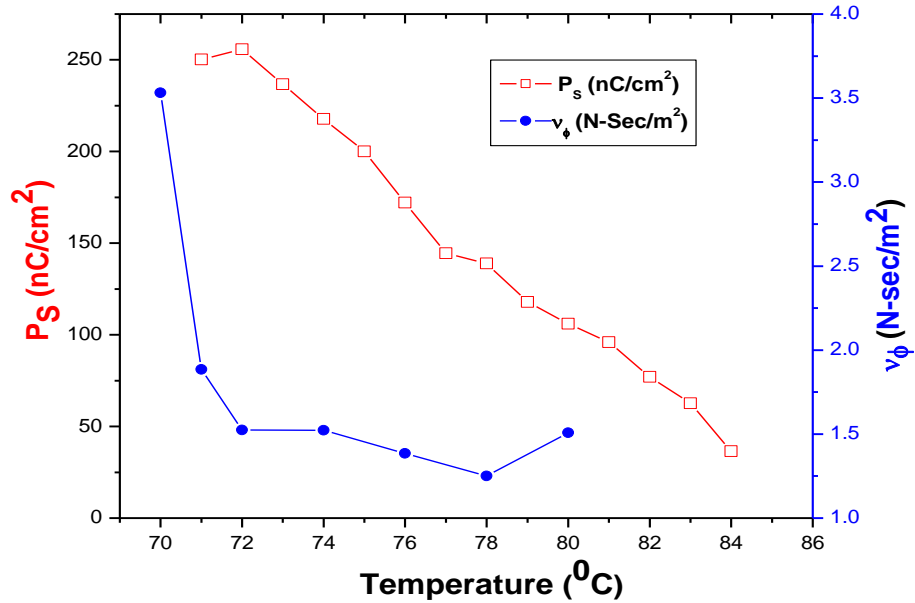


Figure 6.7: Temperature variation spontaneous polarization (P_s) and rotational viscosity γ_ϕ in SmC^* phase.

Using the following relation obtained from the generalized Landau theory [25]

$$\gamma_\phi = \frac{1}{4\pi\epsilon_0} \frac{1}{\Delta\epsilon f_c} \left(\frac{P_s}{\theta} \right)^2$$

it is possible to calculate rotational viscosity, which is related to rotations of the molecular directors about the smectic C^* cone and one of the most important parameters of the SmC^* phase that strongly influences the switchingtime between the field-induced states of FLCs, utilizing spontaneous polarization (P_s), tilt angle (θ), Goldstone mode critical frequency (f_c) and Goldstone mode dielectric strength ($\Delta\epsilon$) (discussed in next section). Temperature variation of calculated rotational viscosity has also been depicted in Figure 6.7. It was found to decrease sharply near SmI^*-SmC^* transition, then it decreases at slower rate and finally shows increasing trend near SmC^*-SmA^* transition which theoretically should diverge.

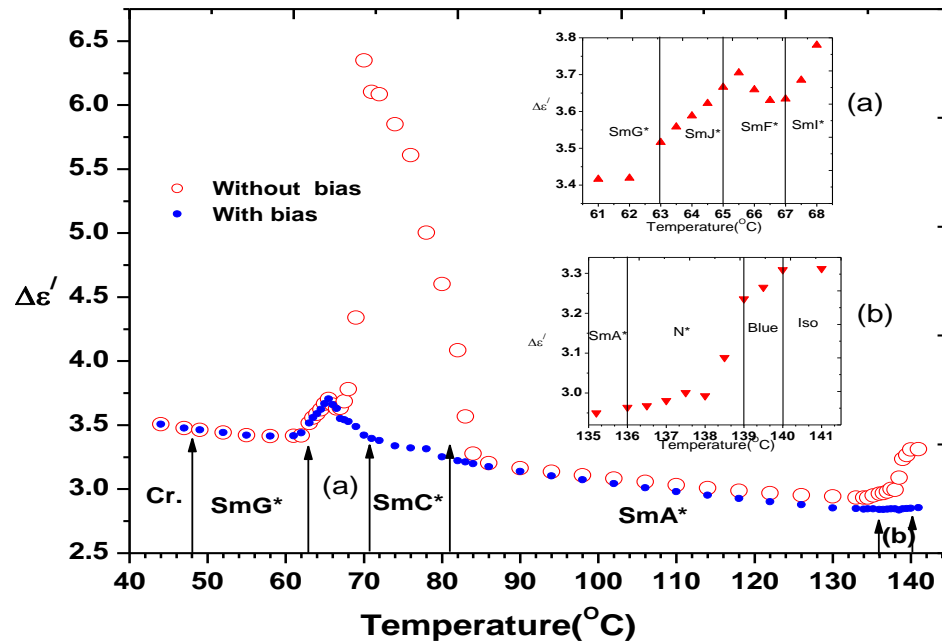


Figure 6.8: Temperature variation of dielectric increment with and without bias field. Magnified views are shown in the inset for (a) in hexatic phases and (b) in cholesteric and blue phases (without bias).

6.4.5 Frequency Dependent Dielectric Study Without Bias

Dielectric behavior of the compound has also been investigated in detail to study the dynamics of the molecules. Dielectric increment ($\Delta\epsilon$) exhibits discontinuous change at all the phase transitions as depicted in Figure 6.8. Transition temperatures between phases differ slightly from those observed from texture and dielectric study. Although long range BOO is established in SmG^* phase along with the establishment of a helical structure but in the measuring cell the helical structure may be suppressed due to strong surface interactions (observed texture supports this), so there might not be appreciable change in $\Delta\epsilon$ at Cr- SmG^* transition as observed and it decreases slightly with increasing temperature. On further heating, when SmJ^* phase is formed where molecular tilt changes from the side of the pseudo-hexagonal net towards the apex, reorientation of the director results in higher tilt and higher $\Delta\epsilon$. At SmJ^* - SmF^* transition since the tilt direction reverses, $\Delta\epsilon$ slightly decreases. On further heating at SmF^* - SmI^* transition tilt direction again changes from the side of the hexagon to apex, $\Delta\epsilon$ again increases. Due to

increased thermal energy, overcoming surface energy helical structure is established in SmC^* phase, greater director reorientation is possible as a result of reduced BOO and reduced coupling between local tilt and bond directions thus generating higher values of $\Delta\varepsilon$ in this phase. However, since molecular tilt in SmC^* is quite small (about 19° at the onset of SmC^* as obtained from optical study) and decreases rapidly with increasing temperature, $\Delta\varepsilon$ is found to decrease quite strongly with temperature. Within SmA^* phase $\Delta\varepsilon$ is small and decreases slightly with temperature. At the onset of cholesteric phase, since helical structure is established again, $\Delta\varepsilon$ increases, although the value is smaller than those observed in low temperature smectic phases because of the absence of the layered structure. On the formation of blue phase $\Delta\varepsilon$ increases further, showing a distinct discontinuity, since in blue phase double twist structure is established from a single twist structure in cholesteric phase.

From the absorption spectra one low frequency collective relaxation process is observed in all the tilted smectic phases except in SmG^* phase. In SmJ^* the process is very weak and the relaxation frequency remains constant with temperature at around 300Hz as shown in Figure 6.9. In SmF^* phase it increases rapidly up to 700Hz. In SmI^* phase it again remains constant at 800 Hz. In SmC^* phase the relaxation frequency again increase with temperature reaching up to 1400 Hz which is identified as Goldstone mode or phason mode associated with fluctuations of the phase angle of the director. One high frequency relaxation process is also observed in hexatic tilted phases which remain almost constant with temperature. On approaching SmC^* - SmI^* (or SmF^*) transition from above two collective director relaxation processes are discussed [26] – higher frequency one is related to amplitude fluctuation whereas the lower frequency one is related to the phase fluctuation of the bond orientational order (BOO) coupled with the polarization and tilt of the molecules. It has been predicted that BOO phason frequency should jump to a lower value at the transition and continue to decrease slowly with decreasing temperature. However, BOO amplitudon mode frequency should jump to a higher value at the transition and continue to increase strongly with decreasing temperature. No such theoretical prediction is available for the dynamic behavior of molecules in SmJ^* and SmG^* phases. Observed temperature variation of BOO related phason frequency in the vicinity of SmC^* - SmI^* transition of MPOBC is as predicted. But BOO amplitudon frequency was observed in all the tilted hexatic phases, it remains almost constant at 420 kHz instead of increasing with decreasing temperature and this mode persists even in SmC^* phase near transition. For a substance denoted

as C8OCOOC5, similar behavior of BOO phason frequency was reported and no amplitude mode was observed in that system [27]. Soft mode could be detected in SmA* phase which increases with temperature from 130 kHz to 200 kHz. No molecular mode was possible to detect in the cholesteric or blue phase because either the mode is very weak or merged with the ITO peak, or the molecular mode in these phases are beyond the frequency measuring range.

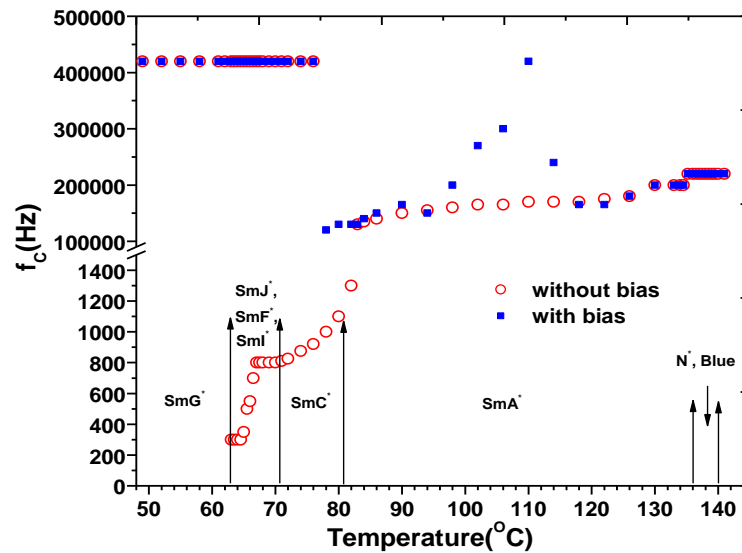


Figure 6.9: Observed critical frequencies with and without bias field in different phases of MPOBC.

6.4.6 Frequency Dependent Dielectric Study With Bias

Relaxation behavior was also studied by applying a dc bias field in addition to the measuring field. At all transitions discontinuous change is observed in dielectric increment ($\Delta\epsilon$) as was observed without bias (Figure 6.8). However, dielectric increment with bias is observed to be less throughout the mesomorphic range as expected. Within SmA* phase it increases with decreasing temperature at substantially higher rate compared to non-bias case. It increases further in SmC* phase and unlike in the without bias situation it continues to increase in SmI* and SmF* phases as has been observed in compound C8OCOOC5 [27]. In SmJ* phase $\Delta\epsilon$ decreases when

temperature is lowered, similar behaviour is observed also in SmG* phase initially, but it increases slightly on further cooling.

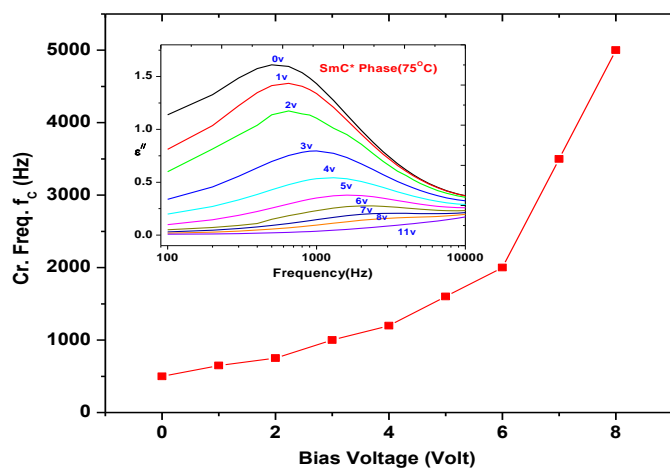


Figure 6.10: Effect of bias voltage on GM critical frequency in SmC* phase (75°C)

In SmC* phase Goldstone mode contribution to dielectric constant decreases with increasing bias field and at about 10 V Goldstone mode was completely suppressed which means that helicoidal structure is completely unwound at that voltage (Figure 6.10, inset). However with increasing bias Goldstone mode critical frequency increases from 500 Hz to about 5 kHz as depicted in Figure 6.10. This might be due to the fact that unwinding of helicoidal structure with bias hinders cooperative phase fluctuations of the molecules.

No BOO related phason mode was observed in the hexatic phases under bias field, however BOO amplitudon mode critical frequency remained similar to that observed without bias (Figure 6.9). In SmA* phase soft mode relaxation frequency was found to increase from 130 kHz (82°C) to 420 kHz (110°C), then decreased to 165 kHz at 118°C and again increased to 200 kHz (130°C), whereas it increased smoothly 130 kHz (82°C) to 200 kHz (130°C) in without bias case. No plausible explanation is available yet for this anomalous behavior.

6.5 CONCLUSION

Phase behaviour, structure and molecular dynamics of the chiral liquid crystalline compound MPOBC have been investigated by optical polarizing microscopy, small and wide angle diffraction by synchrotron radiation and frequency dependent dielectric spectroscopy techniques. Compound exhibits richly polymorphic mesomorphic behavior within 48⁰C to 140⁰C. Other than crystalline and isotropic phases, it shows four tilted hexatic smectic phases (SmG*, SmJ*, SmF*, SmI*), one tilted synclinic SmC* phase, one normal smectic phase (SmA*) along with cholesteric (N*) and a blue phase (BP*). Difference in textures, which reveal topological defect structure, in SmG* and SmJ* phases and those of SmF* and SmI* is subtle. Clear evidence of helicoidal structure in the form of disclination lines is observed in SmI* and in SmC*. Blue coloured platelet texture is observed in BP* phase. Although no hexagonal symmetry was directly revealed from synchrotron study in the hexatic phases but these phases could be distinguished from the wide angle diffraction peak and its satellite structures and measuring the correlation lengths across and within the smectic layers. However, direct evidence of change of tilt direction of the molecules from the edge of the pseudo-hexagonal net (SmF*) towards its apex (SmI*) was observed. In blue phase, correlation length along the director increased substantially to 134 nm from 113 nm in cholesteric phase. Clear discontinuities were observed at the transitions of all the phases in d₀₀₁ smectic layer spacing. Discontinuities were also observed in molecular tilts measured from diffraction and optical methods. Present study nicely depicted the temperature evolution of the different smectic phases along with cholesteric and blue phase in a single compound. Although from mechanics calculation dipole moment of the molecules was found to be rather low (2.06 Debye), the compound exhibited high spontaneous polarization (237 nC/cm²) in ferroelectric SmC* phase. Frequency dependent dielectric spectroscopic study also revealed discontinuous changes in dielectric increment at all the phase transitions. In hexatic phases dielectric absorption spectra revealed one low frequency relaxation process, related to the phase fluctuation of the bond orientational order, and one high frequency process related to amplitude fluctuation of the bond orientational order coupled with the polarization and tilt of the molecules. In SmC* phase Goldstone mode relaxation and in SmA* phase soft mode relaxation processes were detected. Dielectric increment with bias field was found to be less throughout the mesomorphic range compared to non-bias value. Helicoidal structure in SmC* phase could be completely unwound at 10 V bias.

6.6 REFERENCES

- [1] D. Demus and J. Goodby, Handbook of Liquid Crystals, Wiley-VCH Weinheim, (1998).
- [2] P. S. Pershan, Structure of Liquid Crystal Phases, World Scientific Singapore, (1988).
- [3] R. B. Meyer, L. Liebert, L. Strzelecki, P. Keller; J. Phys. (France) Lett., 36, L-69 (1975), Ferroelectric liquid crystals.
- [4] N. A. Clark and S. T. Lagerwall; Appl. Phys. Lett., 36, 899 (1980), Submicrosecond bistable electro-optic switching in liquid crystals.
- [5] D. C. Wright and N. D. Mermin; Rev. Mod. Phys., 66, 385 (1989), Crystalline liquids: the blue phases.
- [6] C. J. F. Botcher and P. Bordewijk; Theory of Electric Polarization Vol. I Elsevier, Amsterdam (1978).
- [7] Wrobel S, Dielectric relaxation spectroscopy, Relaxation phenomena — Liquid crystals, magnetic systems, polymers, high-TC superconductors, metallic glasses, Haase W. and Wrobel S Eds., Ch 1 Springer-Verlag Berlin-Heidelberg (2003).
- [8] D. Goswami, D. Sinha, A. Debnath, P.K. Mandal, S. K. Gupta, W. Haase, D. Ziobro and R. Dabrowski; J. Mol. Liq., 182, 95-101 (2013), Molecular and dynamical properties of a perfluorinated liquid crystal with direct transition from ferroelectric SmC* phase to isotropic phase.
- [9] K. Miyasato, S. Abe, H. Takezoe, A. Fukuda and E. Kuze; Jpn. J. Appl. Phys., 22, L661 (1983), Direct Method with Triangular Waves for Measuring Spontaneous Polarization in Ferroelectric Liquid Crystals.
- [10] P. K. Mandal, B. R. Jaishi, W. Haase, R. Dabrowski, M. Tykarska and P. Kula; Phase Trans., 79, 223-235 (2006), Optical microscopy, DSC and dielectric relaxation spectroscopy studies on a partially fluorinated ferroelectric liquid crystalline compound MHPO(13F)BC.
- [11] I. Dierking, Textures of Liquid Crystals Wiley-VCH, Weinheim, (2003).

- [12] A. J. Leadbetter, J. P. Gaughan, B. Kelly, G. W. Gray and J. Goodby; *J Phys. (France) Colloq.*, 40, C3-178 (1979), Characterisation and structure of some new smectic phases.
- [13] G. W. Gray and J. W. Goodby *Smectic Liquid Crystals, Textures and Structures*, Leonard Hill, Philadelphia, (1984).
- [14] P. A. C. Gane, A. J. Leadbetter and P. G. Wrighton; *Mol. Cryst. Liq. Cryst.*, 66, 247 (1981), Structure and Correlations in Smectic B, F and I Phases.
- [15] H. Stegmeyer, T. Blumel, K. Hiltrop, H. Onnusseit and F. Porsch; *Liq. Cryst.* 1, 3-28 (1986), Thermodynamic, structural and morphological studies on liquid-crystalline blue phases.
- [16] Jan P. F. Lagerwall, Per Rudquist, Sven T. Lagerwall and Frank Gießelmann; *Liq. Cryst.*, 30 399-414 (2003), On the phase sequence of antiferroelectric liquid crystals and its relation to orientational and translational order.
- [17] S. B. Dierker and R. Pindak; *Phys. Rev. Lett.*, 59, 1002 (1987), Dynamics of thin tilted hexatic liquid crystal films.
- [18] E. B. Sirota, P. S. Pershan, L. B. Sorensen and J. Collett; *Phys. Rev. Lett.*, 55, 2039 (1985), X-Ray Studies of Tilted Hexatic Phases in Thin Liquid-Crystal Films.
- [19] E. Grelet, B. Pansu, M-H Li and H. T. Nguyen; *Phys. Rev. Lett.*, 86, 3791 (2001), Structural Investigations on Smectic Blue Phases.
- [20] T. Uemura, Y. Ouchi, K. Ishikawa, H. Takezoe and A. Fukuda; *Jpn. J Appl. Phys.*, 24, L224 (1985), Optical Microscope Observation of Hexagonal Ordering in Surface Stabilized Ferroelectric Liquid Crystal Cells.
- [21] D. Ziobro, R. Dąbrowski, M. Tykarska, W. Drzewiński, M. Filipowicz, W. Rejmer, K. Kuśmierek, P. Morowiak and W. Piecek; *Liq. Cryst.*, 39, 1011 (2012), Synthesis and properties of new ferroelectric and antiferroelectric liquid crystals with a biphenyl benzoate rigid core.
- [22] W. Piecek, Z. Raszewski, P. Perkowski, J. Przedmojski, J. Kedzierski, W. Drzewinski, R. Dabrowski and J. Zielinski; *Ferroelectrics*, 310, 125 (2004), Apparent Tilt Angle and Structural

Investigations of the Fluorinated Antiferroelectric Liquid Crystal Material for Display Application.

[23] J. P. F. Lagerwall, A. Saipa, F. Giesselmann and R. Dabrowski; *Liq. Cryst.*, 31, 1175 (2004), On the origin of high optical director tilt in a partially fluorinated orthoconic antiferroelectric liquid crystal mixture.

[24] A. Mikułko, M. Wierzejska, M. Marzec, S. Wrobel, J. Przedmojski and W. Haase; *Mol. Cryst. Liq. Cryst.*, 477, 185 (2007), Ferroelectricity of Hexatic Phases.

[25] T. Carlsson, B. Zeks, C. Filipic, A. Levstik; *Phys. Rev. A*, 42, 877 (1990), Theoretical model of the frequency and temperature dependence of the complex dielectric constant of ferroelectric liquid crystals near the smectic-C*–smectic-A phase transition.

[26] M. Glogarova and I. Rychetsky; *Dielectric relaxation spectroscopy, Relaxation phenomena — Liquid crystals, magnetic systems, polymers, high-TC superconductors, metallic glasses*, W. Haase and S. Wrobel, Eds., Ch 5.3 Springer-Verlag Berlin-Heidelberg (2003).

[27] I. Rychetsky, D. Pocięcha, V. Dvorak, J. Mieczkowski, E. Gorecka and M. Glogarova; *J. Chem. Phys.*, 111, 1541 (1999), Dielectric behavior of ferroelectric liquid crystals in the vicinity of the transition into the hexatic phase.